EIS and Ac-Electrogravimetry Study of PB Films in KCl, NaCl, and CsCl Aqueous Solutions

José J. García-Jareño,*,† David Giménez-Romero,† Francisco Vicente,† Claude Gabrielli,‡ Michel Keddam,‡ and Hubert Perrot‡

Department Química-Física, Fac. Químicas, Universidad de Valencia, C/ Dr Moliner 50, 46100 Burjassot (Spain) and UPR 15 du CNRS, Physique des Liquides et Electrochimie, 4 Place Jussieu, 75252 Paris (France)

Received: May 20, 2003; In Final Form: July 24, 2003

Prussian Blue films have been studied by means of ac-electrogravimetry, electrochemical impedance spectroscopy, and electrochemical quartz crystal microbalance in different aqueous salt solutions. Impedance data was interpreted in terms of a model based on a potential drop at the electrode/film interface and a potential drop at the film/solution interface. Quantitative results obtained by the fitting of impedance and ac-electrogravimetry allow to conclude that the main contribution to the potential drop at the film/solution interface is due to the dehydration-hydration process of cations on entering or leaving the film.

Introduction

In the last years, impedance spectroscopy has proved to be one of the most powerful techniques in the study of charge transport processes through electroactive films. The simplest models that are used to interpret impedance spectra for electroactive films are based on the single pore model of De Levie[1] or diffusion equivalent models which have been largely used in the description of the behavior of many conducting polymers. However, these models are not always capable of reproducing the transition between the high frequencies region and the low frequencies region in the impedance spectra. That is a very interesting point to be analyzed, since a nonideal behavior of impedance data in conducting polymers at low frequencies has been related with several factors such as the existence of several processes,[2,3] inhomogeneous films,[4] or many other causes.[5−7] In this paper, this nonconcordance will be analyzed by means of a model based on Figure 1 for Prussian Blue films studied by EIS and ac-electrogravimetry.

The Film: Prussian Blue. Prussian Blue (ferric forrocyanide, PB) films are easy to be prepared on the surface of different electrodes and present good electrical properties and an ordered structure which makes these films one of the most studied systems.[8−18]

Prussian Blue can be obtained by different ways. However, when PB films are galvanostatically produced following the procedure described by Itaya et al,[10] it is possible to control the amount and the degree of order in the cristalline structure of the film.[19−21]

According to the results of Mortimer and Rosseinsky,[12,13] PB films freshly deposited are in the "insoluble" form, $Fe_4[Fe(CN)_6]_3$, and after several voltammetric cycles in KCl solutions, PB changes to the "soluble" structure, which is characterized by the presence of potassium substituting 1/4 of the high spin iron sites in the "insoluble" PB structure ($KFeFe(CN)_6$).

One of the most attractive properties of PB films is their electrochromism. PB films can be reduced to the colorless form called Everitt's Salt ($KFe_4[Fe(CN)_6]_3$ or $K_2FeFe(CN)_6$, ES), or oxidized to the yellow form called Prussian Yellow ($KFeFe(CN)_6Cl$ or $FeFe(CN)_6$, PY). These electrochemical processes can be easily detected by cyclic voltammetry of PB films in KCl solution. The reduction process for the "soluble" PB structure in acid aqueous solutions has been described as[10]

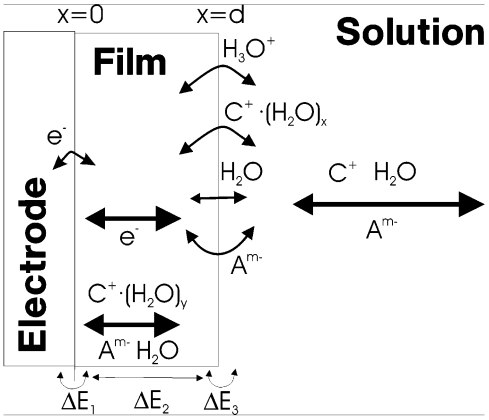

Figure 1. Scheme of the electrode/electroactive film/solution system.

$$\underset{\text{PB}}{KFe^{III}Fe^{II}(CN)_6} + K^+ + e^- \underset{k_c}{\overset{k'_c}{\rightleftharpoons}} \underset{\text{ES}}{K_2Fe^{II}Fe^{II}(CN)_6} \qquad \text{(i)}$$

where Fe^{III} and Fe^{II} refer to the different oxidation states of Fe atoms in the PB structure.

The impedance spectra[21−23] and voltammetric response[9−15,17,24] of PB films in KCl solutions has been the subject of many papers in the last years. However, many aspects are not yet clarified about the electrochemical behavior of these films, especially those concerning the entry and exit of ions and solvent into/from the PB film.

According to the reaction described in scheme i, the reduction of PB to the ES form is accompanied by the entrance of K^+ or other salt cation present in the solution to maintain the electroneutrality. However, the insertion or expulsion of ions from the film can also be accompanied by an exchange of solvent molecules between the film and the outer solution.

This work is aimed at studying and analyzing the electrochemical response of PB films in different aqueous media by various techniques. Differences obtained will be explained in terms of difficulty to change the hydration state of different cations that can participate during these processes.

* To whom correspondence should be addressed. E-mail: jgjareno@uv.es.
† Universidad de Valencia.
‡ Physique des Liquides et Electrochimie.

10.1021/jp035387h CCC: $25.00
Published on Web 09/17/2003

Theory. Figure 1 shows the possible processes of insertion and transport of charged and noncharged species through PB films when reaction i takes place.

These processes are (from left to right):

1. Charge (electron) transfer at the interface electrode/film ($x = 0$). Ions and solvent cannot move through this interface.
2. Transport of species through the film.
2.1. Transport of electrons between the interface electrode/film and the interface film/solution ($x = d$).
2.2. Transport of ions and water (solvent) through the film.
3. Insertion or expulsion of ions and water at the interface film/solution. Electrons do not move through this interface.
4. Transport of ions and water in the solution.

It is considered that species move through the outer solution fast enough not to control the rate of the overall process. Then, there are three possible potential steps according to this scheme: at the electrode/film interface (ΔE_1), through the film (ΔE_2) and at the film/solution interface (ΔE_3). Then, faradaic impedance can be written as

$$Z_F = \frac{\Delta E_1}{\Delta I_F} + \frac{\Delta E_2}{\Delta I_F} + \frac{\Delta E_3}{\Delta I_F} \tag{1}$$

From this hypothesis, it is possible to write an expression for the flux of different charged species at interface electrode/film and interface film/solution[25−32]

$$\frac{\Delta J_{e-}}{\Delta E_1}(x=0) = \frac{G_{e-}}{1 + K_{e-}\dfrac{\coth(d\sqrt{j\omega/D_{e-}})}{\sqrt{j\omega D_{e-}}}} \tag{2}$$

Expression for the flux of electrons at the electrode/film interface, because it is assumed that no other species can move through this interface. D_{e-} represents an apparent diffusion coefficient for electrons through the PB film, d is the film thickness, and K_e and G_e are defined as

$$K_e = k_e^0 \exp(b_e(E - E_e^{\,0})) - k_e^{0\prime}\exp(b_e'(E - E_e^{\,0})) \cdot C_e(x=0) \tag{3}$$

$$G_e = b_e k_e^0 \exp(b_e(E - E_e^{\,0})) \cdot (C_e - C_{e,min}) - b_e' k_e^{0\prime}\exp(b_e'(E - E_e^{\,0})) \cdot C_e(x=0) \cdot (C_{e,max} - C_{e,min}) \tag{4}$$

where

$$b_e = \frac{n\alpha_e F}{RT} \text{ and } b_e' = -\frac{n\beta_e F}{RT} \tag{5}$$

E_e^0 represents a normal potential for the electron-transfer reaction, $C_e(x = 0)$ represents a concentration of active sites for electron transfer at the electrode surface, $C_{e,max}$ and $C_{e,min}$ represent the maximum and minimum concentrations available for electron insertion in the film, respectively, and C_e is the concentration of electrons inserted in the film.

The process of charge compensation during the PB⇆ES reduction takes place by the main participation of salt cations and hydrated protons.[31,33] Then, at the film/solution interface, the flux of these cations can be expressed as

$$\frac{\Delta J_i}{\Delta E_3}(d) = \frac{G_i}{1 + K_i\dfrac{\coth(d\sqrt{j\omega/D_i})}{\sqrt{j\omega D_i}}} \tag{6}$$

where the subscript i makes reference to the salt cations (c^+) and the hydrated proton (H_3O^+) species. D_i represents the diffusion coefficients for the i species through the PB film.

If it is supposed that the film is thin enough, then ΔE_2 can be considered negligible if compared with ΔE_1 and ΔE_3. That way, the faradaic impedance can be written as

$$Z_F \approx Z_1 + Z_3 = \frac{1}{FG_e}\left[1 + K_e\frac{\coth(d\sqrt{j\omega/D_e})}{\sqrt{j\omega D_e}}\right] + \frac{1}{\dfrac{1}{FG_{c^+}}\left[1 + K_{c^+}\dfrac{\coth(d\sqrt{j\omega/D_{c^+}})}{\sqrt{j\omega D_{c^+}}}\right]} + \frac{1}{\dfrac{1}{FG_{H_3O^+}}\left[1 + K_{H_3O^+}\dfrac{\coth(d\sqrt{j\omega/D_{H_3O^+}})}{\sqrt{j\omega D_{H_3O^+}}}\right]} = \frac{1}{FG_e}\left[1 + \frac{K_e\tau_e}{d}\frac{\coth(\sqrt{j\omega\tau_e})}{\sqrt{j\omega\tau_e}}\right] + \frac{1}{\dfrac{1}{FG_{c^+}}\left[1 + \dfrac{K_{c^+}\tau_{c^+}}{d}\dfrac{\coth(\sqrt{j\omega\tau_{c^+}})}{\sqrt{j\omega\tau_{c^+}}}\right]} + \frac{1}{\dfrac{1}{FG_{H_3O^+}}\left[1 + \dfrac{K_{H_3O^+}\tau_{H_3O^+}}{d}\dfrac{\coth(\sqrt{j\omega\tau_{H_3O^+}})}{\sqrt{j\omega\tau_{H_3O^+}}}\right]} \tag{7}$$

In these equations, $\tau_i = d^2/D_i$ represents a time constant, and K_i are related with kinetics constants for the electrochemical reaction[31,32]

$$K_i = k_i + k'_i C_{i,sol} = k_{i0}\exp(b_i(E - E_i^0)) + k'_{i0}\exp(b_i'(E - E_i^0))C_{i,sol} \tag{8}$$

where $C_{i,sol}$ represents the outer concentration of species i and E_i^0, the formal potential.

In these equations, G_i refers to the insertion of ions or electrons transfer at the interface and $G_i < 0$ for inserting species and $G_i > 0$ for expelling species

$$G_i = b_i k_i (C_i - C_{i,min}) - b_i' k_i' (C_{i,max} - C_i) C_{i,sol} \tag{9}$$

where $C_{i,min}$ and $C_{i,max}$ represent minimum and maximum concentration sites available for insertion in the PB film and C_i the concentration of occupied sites in the PB.

The insertion/expulsion law versus potential, $C_i(E)$ is

$$C_i(E) = \frac{C_{i,max}\exp[(b_i' - b_i)(E - E_i^0 - E_i)] + C_{i,min}}{1 + \exp[(b_i' - b_i)(E - E_i^0 - E_i)]} \tag{10}$$

where E_i is defined by

$$C_{i,sol}\frac{k'_{i0}}{k_{i0}} = \exp[-(b_i' - b_i)E_i] \tag{11}$$

The derivative of $C_i(E)$ is equal to

$$\frac{dC_i(E)}{dE} = \frac{b_i - b_i'}{2} \frac{C_{i,max} - C_{i,min}}{1 + \cosh[(b_i' - b_i)(E - E_i^0 - E_i)]} \quad (12)$$

Equations 10−12 are also valid for electrons.[32]

During the past few years, a new technique based on the coupling of EIS and fast EQCM measurements has been developed, namely ac-electrogravimetry. This technique has been successfully used for studies of doping-undoping processes of conducting polymers during electrochemical reactions.[21,28−32,34−38] During these processes, a net flux of water molecules may take place, but it does not modify the faradaic impedance function because it does not represent a net flux of electrical charge. Nevertheless, the ac-electrogravimetric transfer function can be affected. If the solvent enters or leaves the film solvating the cation, then it moves with the same time constant and it makes the apparent molar mass of the cation increase, but if water moves independently of the cation, then their flux should be considered as a new term in the ac-electrogravimetric transfer function.

Subsequently, the ac-electrogravimetric transfer function can be written in terms of flux of species as

$$\frac{\Delta m}{\Delta E_3}(\omega) = -\frac{A}{j\omega}\left[m_{c^+}\frac{\Delta J_{c^+}(d)}{\Delta E_3} + m_{H_3O^+}\frac{\Delta J_{H_3O^+}(d)}{\Delta E_3} + m_s\frac{\Delta J_s(d)}{\Delta E_3}\right] =$$

$$-\frac{A}{j\omega}\left[\frac{m_{c^+}G_{c^+}}{1 + K_{c^+}\dfrac{\coth(d\sqrt{j\omega/D_{c^+}})}{\sqrt{j\omega D_{c^+}}}} + \frac{m_{H_3O^+}G_{H_3O^+}}{1 + K_{H_3O^+}\dfrac{\coth(d\sqrt{j\omega/D_{H_3O^+}})}{\sqrt{j\omega D_{H_3O^+}}}} + \frac{m_{H_2O}G_{H_2O}}{1 + K_{H_2O}\dfrac{\coth(d\sqrt{j\omega/D_{H_2O}})}{\sqrt{j\omega D_{H_2O}}}}\right] =$$

$$-\frac{A}{j\omega}\left[\frac{m_{c^+}G_{c^+}}{1 + \dfrac{K_{c^+}\tau_{c^+}}{d}\dfrac{\coth(\sqrt{j\omega\tau_{c^+}})}{\sqrt{j\omega\tau_{c^+}}}} + \frac{m_{H_3O^+}G_{H_3O^+}}{1 + \dfrac{K_{H_3O^+}\tau_{H_3O^+}}{d}\dfrac{\coth(\sqrt{j\omega\tau_{H_3O^+}})}{\sqrt{j\omega\tau_{H_3O^+}}}} + \frac{m_{H_2O}G_{H_2O}}{1 + \dfrac{K_{H_2O}\tau_{H_2O}}{d}\dfrac{\coth(\sqrt{j\omega\tau_{H_2O}})}{\sqrt{j\omega\tau_{H_2O}}}}\right] \quad (13)$$

where the flux of solvent (water) is also be considered instead of the flux of electrons.

However, this expression does not exactly correspond with the ac-electrogravimetric transfer function $\Delta m/\Delta E$, since $\Delta E = \Delta E_1 + \Delta E_3$. Then, it should be written

$$\frac{\Delta E}{\Delta m} = \frac{\Delta E_1}{\Delta m} + \frac{\Delta E_3}{\Delta m} = \frac{\Delta I_F}{\Delta m}\left(\frac{\Delta E_1}{\Delta I_F} + \frac{\Delta E_3}{\Delta I_F}\right) = -\frac{j\omega\Delta q}{\Delta m}(Z_{F1} + Z_{F3}) = -\frac{j\omega\Delta q}{\Delta m}Z_F \quad (14)$$

where q represents the electrical charge.

Comparison with Transmission Line Models. Each term in eq 7 is mathematically equivalent to those used for interpreting the impedance due to a porous electrode or due to an electroactive film based on transmission line elements.[1,39,40] In these expressions, the faradaic impedance can be written as

$$Z_F = R_{ct} + Z_{TL} = R_{ct} + R_{TL}\frac{\coth(\sqrt{j\omega R_{TL}C_{TL}})}{\sqrt{j\omega R_{TL}C_{TL}}} \quad (15)$$

By comparing eqs 7 and 15 it is found out that

$$\tau_i = R_{TL}C_{TL} = \frac{d^2}{D_i} \quad (16)$$

$$\frac{R_{TL}}{R_{ct}} = \frac{K_i\tau_i}{d} \quad (17)$$

$$G_i = \frac{1}{FR_{ct}} \quad (18)$$

In this model, R_{TL} has the physical meaning of a resistance of transport of species through the film, and C_{TL} represents a distributed capacitance through the walls of the pore. R_{ct} represents a charge-transfer resistance.

Simplifications. Once the more general model is proposed, there are some factors to be analyzed. The first one is the fact that this model allows the good reproduction of the shape of impedance spectra or ac-electrogravimetry obtained for PB films. However, some problems appear when trying to fit experimental data to this model. The most important one is that different parameters can probably reproduce the same curve. That means that the obtained parameters are not independent. Therefore, there are two possible strategies to enlarge the number of degrees of freedom of the fitting. The first is to fix some parameters that can be evaluated or known by other techniques, and the second is to simplify the model.

Two possible simplifications will be discussed now:

(i) Potential drop at the electrode/film interface is negligible, and water does not enter or leaves the film independently of cations.

According to this hypothesis, the impedance spectra function and ac-electrogravimetry reduce to

$$Z_F^{-1} \approx Z_3^{-1} = \frac{1}{\dfrac{1}{FG_{c^+}}\left[1 + \dfrac{K_{c^+}\tau_{c^+}}{d}\dfrac{\coth(\sqrt{j\omega\tau_{c^+}})}{\sqrt{j\omega\tau_{c^+}}}\right]} + \frac{1}{\dfrac{1}{FG_{H_3O^+}}\left[1 + \dfrac{K_{H_3O^+}\tau_{H_3O^+}}{d}\dfrac{\coth(\sqrt{j\omega\tau_{H_3O^+}})}{\sqrt{j\omega\tau_{H_3O^+}}}\right]} \quad (19)$$

$$\frac{\Delta m}{\Delta E} \approx \frac{\Delta m}{\Delta E_3} = -\frac{A}{j\omega}\left[\frac{m_{c^+} G_{c^+}}{1+\frac{K_{c^+}\tau_{c^+}}{d}\frac{\coth(\sqrt{j\omega\tau_{c^+}})}{\sqrt{j\omega\tau_{c^+}}}} + \frac{m_{H_3O^+} G_{H_3O^+}}{1+\frac{K_{H_3O^+}\tau_{H_3O^+}}{d}\frac{\coth(\sqrt{j\omega\tau_{H_3O^+}})}{\sqrt{j\omega\tau_{H_3O^+}}}}\right] \quad (20)$$

According to these equations, six independent parameters are needed for the impedance or ac-electrogravimetry fitting.

(ii) There is only one cation species that participates during electrochemical reaction, and water does not enter or leave the film independently of this cation.

In this case, impedance and ac-electrogravimetry functions reduce to

$$Z_F \approx Z_1 + Z_3 = \frac{1}{FG_e}\left[1+\frac{K_e\tau_e}{d}\frac{\coth(\sqrt{j\omega\tau_e})}{\sqrt{j\omega\tau_e}}\right] + \frac{1}{FG_{c^+}}\left[1+\frac{K_{c^+}\tau_{c^+}}{d}\frac{\coth(\sqrt{j\omega\tau_{c^+}})}{\sqrt{j\omega\tau_{c^+}}}\right] =$$

$$\left[\frac{1}{FG_e}+\frac{1}{FG_{c^+}}\right] + \frac{K_e\tau_e}{FG_e d}\frac{\coth(\sqrt{j\omega\tau_e})}{\sqrt{j\omega\tau_e}} + \frac{K_{c^+}\tau_{c^+}}{FG_{c^+} d}\frac{\coth(\sqrt{j\omega\tau_{c^+}})}{\sqrt{j\omega\tau_{c^+}}} \quad (21)$$

$$\frac{\Delta m}{\Delta E} = -\frac{Am_{c^+}}{Fj\omega Z_F} = -\frac{A}{j\omega}\left[\frac{m_{c^+}}{\left[\frac{1}{G_{c^+}}+\frac{1}{G_e}\right] + \frac{K_{c^+}\tau_{c^+}}{G_{c^+} d}\frac{\coth(\sqrt{j\omega\tau_{c^+}})}{\sqrt{j\omega\tau_{c^+}}} + \frac{K_e\tau_e}{G_e d}\frac{\coth(\sqrt{j\omega\tau_e})}{\sqrt{j\omega\tau_e}}}\right] \quad (22)$$

According to these equations, there are five independent parameters for the impedance and ac-electrogravimetry fitting.

Experimental Section

Prussian Blue films were galvanostatically prepared ($i = -40\mu$A cm^{-2} for 150 s) in 0.02 M $K_3Fe(CN)_6$, 0.02 M $FeCl_3$ and 0.01 M HCl solutions.[9−11] PB films used for the study in NaCl solutions were generated at higher deposition currents ($i = 600\ \mu$A cm^{-2} for 10 s) because its stability strongly increases in these conditions.[10] All the chemicals used (KCl, CsCl, NaCl, and those used for the deposition) were Panreac or Merck analytical reagent (p.a.) except HCl (chemically pure). Before starting electrochemical experiments, these films freshly prepared were cycled around the PB ⇆ ES system for 10 times in the aqueous salt solution where they are studied, because that way a more stable response is obtained.[13] Then the aqueous solution is changed and the films are rinsed.

The electrochemical quartz crystal microbalance takes advantage of the change of the resonance frequency of a 6 MHz "AT-cut" quartz crystal (CQE, Troyes, France) due to a minute mass change of one of its electrodes exposed to solution. Two 0.2 cm^2 gold electrodes were deposited on the opposite faces of the quartz crystal: they allowed the resonator to be electrically connected to an oscillator circuit, whereas the electrode exposed to the solution was used as the working electrode. The frequency change due to an added mass is described by the Sauerbrey's law.[41] The use of this equation to obtain mass from frequency changes has been validated by means of acoustic impedance analysis for this system.[42] An experimental value for the mass/frequency coefficient sensitivity $-7.5\ 10^{+7}$ Hz g^{-1} cm^{+2} was used for the experimental treatment of all the gravimetric data; this coefficient was previously estimated through copper galvanostatic electrodeposition.

To use this fast QCM in the ac mode, the modified working electrode was polarized and a sinusoidal small amplitude potential perturbation was superimposed. The frequency response, Δf, corresponding to the mass modulation, Δm, of the modified working electrode, was measured simultaneously with the current response of the electrode. The resulting signals were sent to a four-channel frequency response analyzer (Solartron 1254), which allowed the electrogravimetric transfer function, $\Delta m/\Delta E$ to be simultaneously obtained with the electrochemical impedance. Then, the faradaic impedance, Z_F, was obtained from electrochemical impedance data by eliminating uncompensated resistance and double layer capacitance contributions.

Fitting of experimental data to the theoretical models proposed was done by means of a least squares "homemade" software based on the Marquardt algorithm for optimization of functions and the J. R. MacDonald weighting for the real and imaginary parts of impedance.[43,44]

Results and Discussion

Cyclic Voltammetry + Quartz Crystal Microbalance. Voltammetry of PB films in different aqueous media is analyzed. Figure 2a shows voltammograms of PB films in KCl, NaCl, and CsCl solutions. Peak potentials, E_p depend on the nature of the cation present in the solution: $E_{p(Cs^+)} > E_{p(K^+)} > E_{p(Na^+)}$. In addition, it has been corroborated that the shape of the first voltammogram of a PB film in a CsCl solution depends on the time that the film has been immersed in.[45,46] This fact has been explained considering that cesium cations can enter the film and move easily through the interface film/solution.

On the other hand, well-defined voltammograms of PB films in NaCl solutions are recorded when films are generated at higher currents or also when a Nafion membrane covers the PB film.[21] This particular behavior has been explained by the need for dehydration of sodium cations before entering the PB film. This hypothesis of previous dehydration is confirmed by analyzing changes in mass obtained by EQCM (Figure 2b). The mass/electrical charge ratio ($F\ \Delta m/\Delta q$) during cathodic or anodic peaks of voltammograms of Figure 2 are 105 g mol^{-1} in CsCl solutions, 22 g mol^{-1} in NaCl solution and 29 g mol^{-1} in KCl solutions. In the case of CsCl and KCl solutions, this value does not correspond exactly to a pure Cs^+ or K^+ participation as countercation. Studies by ac-electrogravimetry and impedance proved that hydrated protons can partially participate during these electrochemical processes, and this fact causes an apparent small atomic mass.[31] In the case of Na^+ cations the difference between the molar mass of cations (23 g mol^{-1}) and the molar mass of hydrated protons (19 g mol^{-1}) is very small, and therefore, molar masses apparently agree with those of the salt cation. Therefore, from these results, it is not possible to confirm whether hydrated protons participate during electrochemical processes in NaCl solutions or not, but it is proved that alkali cations that enter into the PB film are not hydrated.

Studies in other metal-hexacyanoferrates reveal that larger, even divalent cations, can enter or leave films during electro-

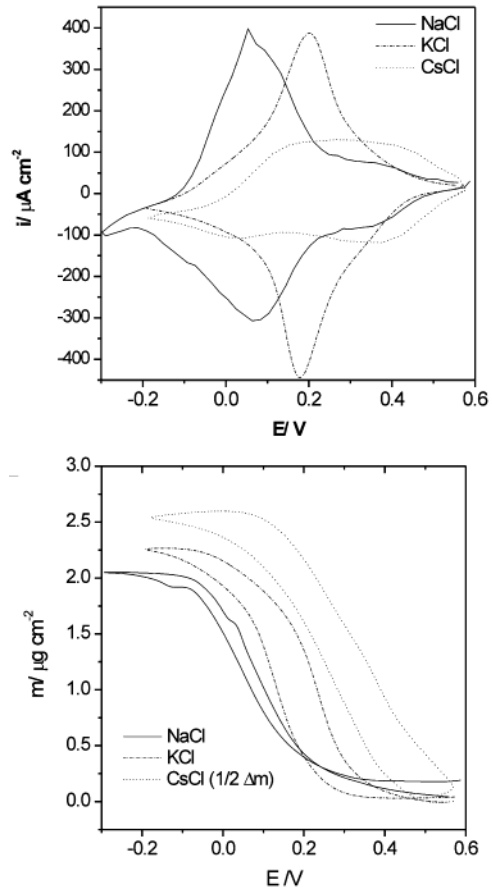

Figure 2. Voltammograms for PB films in NaCl, KCl, and CsCl aqueous solutions (2a) and mass changes associated to these voltammograms (2b). All solutions were 0.5 M, and pH was 2.48−2.78. Scan rate 10 mV s^{-1}.

chemical processes.[47] Studies of Ni-hexacyanoferrates show that the participation of water molecules accompanying the alkali cation seems to be more pronounced than in this case.[48] In Ni-hexacyanoferrates and in KCl solutions, it has also been reported that potassium cations enter or leave the film without water[49] but in solutions containing Cs^+ the smaller values of the mass/charge relationship are attributed to an opposite flux of water during the electrochemical processes.[50]

Electrochemical Impedance Spectroscopy and Ac-Electrogravimetry. Previous studies of EIS of PB films have proved the dependence of conductive properties of films on the pH or the temperature and on the nature of the cation, which is present in the outer aqueous solution.[16,19,22,23]

By ac-electrogravimetry, it has been proved that in acid KCl solutions it is the potassium cation that mainly participates in the charge compensation process. However, there is always a participation of hydrated protons mainly detected at potentials where the electrochemical reduction starts.[31,33]

In this work, a more quantitative analysis of ac-electrogravimetry and EIS data is made in different aqueous solutions.

(*a*) *KCl Solutions.* Figure 3 shows EIS (presented as complex plane capacitance plots) at different potential in an acid KCl solution. These data were fitted to eq 19 that corresponds to the assumption that potential drop at the electrode/film interface is negligible. That way, when trying to fit experimental data to this model a main process (small impedance) and a secondary process (large impedance) are found out, because eq 19 corresponds to a parallel association of elements in an equivalent circuit. Table 1 collects parameters obtained for the main process

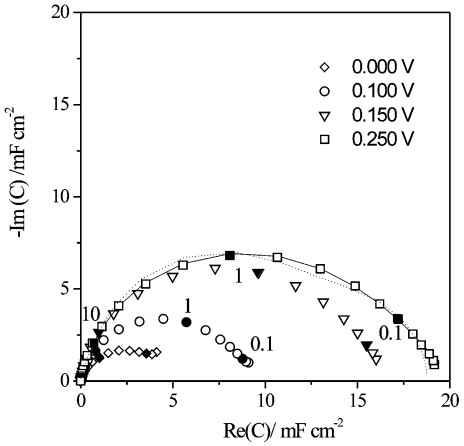

Figure 3. EIS presented as capacitance plots of a PB film at different potentials vs SCE in KCl 0.5 M and pH 2.0 solution. Discontinuous line represents the fitting of experimental data to eq 19, and continuous line represents the fitting of experimental data to eq 23. Parameters used for the fitting of experimental data are collected in Tables 1 and 2.

TABLE 1: Dependence of Parameters Obtained from the Fitting of Impedance Data and Ac-Electrogravimetry Data to Eqs 19 and 20 for a PB Film Immersed in a KCl 0.5 M Solution at Different Potentials against SCE Reference Electrode[a]

	impedance			ac-electrogravimetry		
E (V)	*m*G* (mg $V^{-1}s^{-1}cm^{-2}$)	*K/d* s^{-1}	*τ* (s)	*m*G* (mg $V^{-1}s^{-1}cm^{-2}$)	K/d s^{-1}	*τ* (s)
0.000	0.015	13	0.5	0.010	7	0.5
0.025	0.031	20	0.3	0.021	14	0.3
0.050	0.057	30	0.2	0.018	16	0.1
0.075	0.098	42	0.2	0.071	36	0.2
0.100	0.160	54	0.1	0.120	51	0.1
0.125	0.230	62	0.1	0.160	58	0.1
0.150	0.310	63	0.1	0.240	62	0.1
0.175	0.410	63	0.1	0.350	61	0.1
0.200	0.440	51	0.1	0.340	43	0.2
0.225	0.320	43	0.2	0.250	37	0.2
0.250	0.180	36	0.2	0.150	31	0.2
0.275	0.110	30	0.2	0.086	25	0.2
0.300	0.066	24	0.2	0.053	21	0.3
0.325	0.036	18	0.3	0.022	14	0.3
0.350	0.018	12	0.4	0.011	10	0.6
0.375	0.010	9	0.6	0.003	5	0.7
0.400	0.006	7	0.7	0.001	5	0.8

[a] *G* parameter in impedance data is multiplied by the molar mass of potassium cations (38.9 g mol^{-1}) to make it comparable with the value obtained from ac-electrogravimetry.

because parameters obtained for the secondary process do not follow a clear trend and are affected by larger errors.

Figure 4 shows ac-electrogravimetry for a PB film in an acid KCl solution at several potentials. The shape of this plot is always a semicircle on the third quadrant and indicates the participation of cations as counterions.[31] The width of this loop depends on the applied potential being maximum at potentials near the redox potential. Fitting of ac-electrogravimetry experimental data to the theoretical model proposed in eq 20 leads to similar parameters of those obtained for EIS fitting (Table 1).

The analysis of the variation of these parameters on the potential shows that, according to the model, G_c parameters are maximum at potentials near the redox potential of the PB⇆ES process. Also, the time constants, τ_c, for this process are minimum at these potentials. These variations are fully consistent with the model proposed.

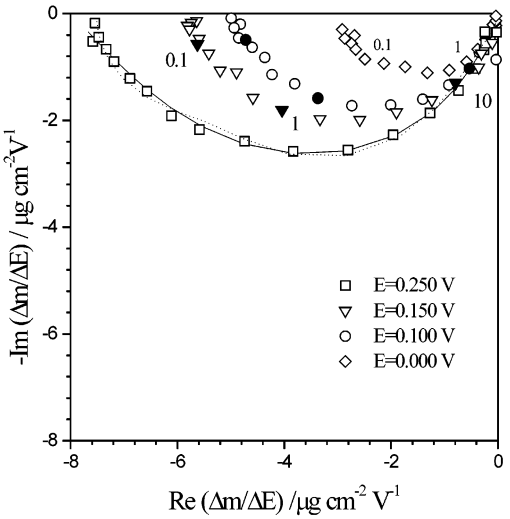

Figure 4. Ac-electrogravimetric transfer function of a PB film at different potentials vs SCE in KCl 0.5 M and pH 2.0 solution. Discontinuous line represents the fitting of experimental data to eq 20, and continuous line represents the fitting of experimental data to eq 24. Parameters used for the fitting of experimental data are collected in Tables 1 and 2.

Nevertheless, according to the predictions of this model and assuming a Butler−Volmer like dependence of kinetics constants on the potential (equation 8), K_c should be minimum at formal potentials of the redox process. However, maximum values here are obtained for this parameter (K_c/d) at these potentials. Therefore, there is something in these simplifications that is made wrong. In fact, this model does not consider the coupled movement of electron and cations during the electrochemical processes. This case has been treated in the literature by different strategies such as a binary diffusion of PB and ES,[51] transmission line models including paths for both electron and ions transport,[1,52−54] and the Vorotyntsev et al.[6] or Buck et al.[55] models, in which local electroneutrality condition is imposed.

Now, these results were analyzed by making use of the other simplification proposed in the theory section: Only one cation species, but potential drop at the electrode/film interface, is not negligible, and the local electroneutrality condition is not imposed.[32] That way, EIS and ac-electrogravimetry data were fitted to eqs 21 and 22. Although this fitting is possible, values for τ and K/dG for one of the two processes are not independent. This is caused by the fact that τ proves large enough (>100 s), and in these conditions, the hyperbolic cotangent term can be simplified to the unity (for frequencies = 0.02 Hz, the error is about 2% in this term, and for frequencies = 0.05 Hz, error is only about 0.1%). Then, the term corresponding to the apparent diffusion of electrons becomes a Warburg-like impedance, and equations for the faradaic impedance and ac-electrogravimetry remain as

$$Z_F \approx Z_1 + Z_3 = \left(\frac{1}{FG_e} + \frac{1}{FG_{c^+}}\right) + \left[\frac{K_e\tau_e}{FdG_e}\frac{\coth(\sqrt{j\omega\tau_e})}{\sqrt{j\omega\tau_e}} + \frac{K_{c^+}\tau_{c^+}}{FdG_{c^+}}\frac{\coth(\sqrt{j\omega\tau_{c^+}})}{\sqrt{j\omega\tau_{c^+}}}\right] = \left(\frac{1}{FG_e} + \frac{1}{FG_{c^+}}\right) + \frac{K_{c^+}\tau_{c^+}}{FdG_{c^+}}\frac{\coth(\sqrt{j\omega\tau_{c^+}})}{\sqrt{j\omega\tau_{c^+}}} + \frac{K_e\sqrt{\tau_e}}{FdG_e}\frac{1}{\sqrt{j\omega}} \quad (23)$$

$$\frac{\Delta m}{\Delta E} = -\frac{A}{j\omega}\left[\frac{m_{c^+}}{\frac{1}{G_{c^+}}\left(1 + \frac{K_{c^+}\tau_{c^+}}{d}\frac{\coth(\sqrt{j\omega\tau_{c^+}})}{\sqrt{j\omega\tau_{c^+}}}\right) + \frac{1}{G_e}\left(1 + \frac{K_e\tau_e}{d}\frac{\coth(\sqrt{j\omega\tau_e})}{\sqrt{j\omega\tau_e}}\right)}\right] = -\frac{A}{j\omega}\left[\frac{m_{c^+}}{\left(\frac{1}{G_{c^+}} + \frac{1}{G_e}\right) + \left(\frac{K_{c^+}\tau_{c^+}}{dG_{c^+}}\frac{\coth(\sqrt{j\omega\tau_{c^+}})}{\sqrt{j\omega\tau_{c^+}}}\right) + \left(\frac{K_e\sqrt{\tau_e}}{dG_e}\frac{1}{\sqrt{j\omega}}\right)}\right] \quad (24)$$

That way, the four independent parameters that can be evaluated from the fitting are $(1/G_{c^+} + 1/G_{e^-})$, K_{c^+}/dG_{c^+}, τ_{c^+}, and $(K_e\sqrt{\tau_e})/dG_e$. It is considered that the slowest process is the electron transport through the PB film. It is mathematically equivalent to assuming that cations transport is the slowest process. This assumption will be discussed later.

Figures 3 and 4 show experimental EIS and ac-electrogravimetry at E = 250 mV, near the redox potential of the PB⇆ES process, the obtained fitting by considering that two species participate during the charge compensation process (fitting 1, eqs 19 and 20), and the obtained fitting by considering that only one cation participates and that the rate of flux of electrons also affects it (fitting 2, eqs 23 and 24). Both fittings give good simulation curves, but better for fitting 2. Even the number of parameters used is smaller in fitting 2 and reproduces better experimental data than fitting 1.

Table 2 collects values obtained from the fitting of EIS and ac-electrogravimetry to these functions. It is important to note that parameters obtained by the fitting of ac-electrogravimetry and EIS are not very different. By analysis of the dependence of these parameters on the potential, it is observed that $(1/G_{c^+} + 1/G_e)$ is minimum at redox potentials, K_{c^+}/dG_{c^+}, which represents the inverse of the derivative of the insertion law for potassium cations,[21,29] is also minimum at these potentials, and the time constant, τ_{c^+}, also proves minimum at these potentials. The other term calculated, $(K_e\sqrt{\tau_e})/dG_e$, is also minimum at redox potentials. All these dependences can be explained by this model.

Besides, by analyzing the dependence on the potential of $(1/G_{c^+} + 1/G_e)$ it is possible to obtain values for the b and b' parameters (eq 5), which are 20.0 V^{-1} and −22.9 V^{-1}, which correspond at 298 K to $\alpha = 0.51$ and $\beta = 0.59$, respectively.

These results are consistent with the shape of voltammograms in KCl solutions, where a reversible peak is obtained.

(*b*) *NaCl Solutions.* PB films generated at higher deposition currents[19,21] have been studied in acid NaCl solutions by EIS and ac-electrogravimetry. Figures 5 and 6 show EIS and ac-electrogravimetry both at E = 100 mV, the formal potential in NaCl solutions for the PB⇆ES process. The first analogy that can be observed, if compared with experiments in KCl solutions, is that ac-electrogravimetry also corresponds to a semicircle on the third quadrant, which means a main contribution of cations to the charge compensation process. On the other hand, the ratio $F\,\Delta m/\Delta q = F\,\Delta m/\Delta E\;\Delta E/\Delta I_F = F\,\Delta m/\Delta E\;Z_F$ gives a value near 23 g mol^{-1} in a wide range of frequencies. That means that sodium cations enter or leave the film without water accompanying the cation. Then, experimental data were fitted to the same theoretical equations (23 and 24), and values obtained for the different parameters are collected in Table 3. Although values obtained by fitting EIS and ac-electrogravi-

TABLE 2: Dependence of Parameters Obtained from the Fitting of Impedance Data and Ac-Electrogravimetry Data to Eqs 23 and 24 for a PB Film Immersed in a KCl 0.5 M Solution at Different Potentials against the SCE Reference Electrode

	impedance				ac-electrogravimetry			
E (V)	$1/FG_e + 1/FG_{c^+}$ (Ω cm^2)	$K_{c^+}/G_{c^+}d$ (V cm^2 μmol^{-1})	τ_{c^+}	$(K_e\sqrt{\tau_e})/dG_e$ (V cm^2 s$^{1/2}$ μmol^{-1})	$1/FG_e + 1/FG_{c^+}$ (Ω cm^2)	$K_{c^+}/G_{c^+}d$ (V cm^2 μmol^{-1})	τ_{c^+}	$(K_e\sqrt{\tau_e})/dG_e$ (V cm^2 s$^{1/2}$ μmol^{-1})
0.000	26	19	0.7	6	37	18	0.3	6
0.025	13	16	0.3	5	17	15	0.2	5
0.050	7	15	0.2	2	8	15	0.2	2
0.075	4	12	0.1	2	5	12	0.1	2
0.100	3	10	0.1	2	3	11	0.1	2
0.125	2	8	0.1	1	2	9	0.1	1
0.150	1	6	0.1	1	2	6	0.1	1
0.175	1	4	0.0	1	1	4	0.1	1
0.200	1	3	0.1	1	1	3	0.1	1
0.225	1	3	0.1	1	2	4	0.1	1
0.250	2	5	0.1	1	2	5	0.1	1
0.275	4	7	0.1	2	4	7	0.1	2
0.300	6	8	0.1	3	8	9	0.2	3
0.325	11	10	0.2	4	14	13	0.3	4
0.350	22	13	0.3	6	32	19	0.4	8
0.375	43	16	0.4	10	45	23	0.8	11
0.400	66	18	0.5	14	68	24	1.6	7

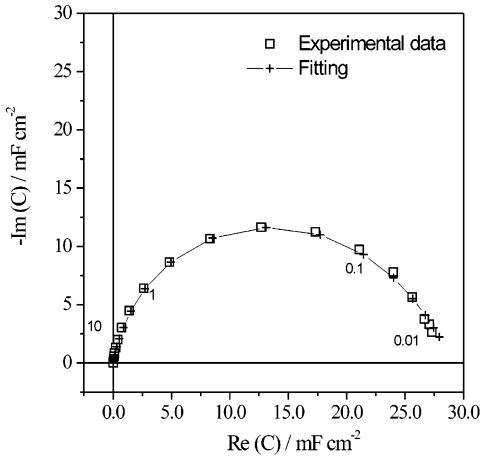

Figure 5. EIS presented as capacitance plots of a PB film at $E = +0.100$ V vs SCE in NaCl 0.5 M and pH 2.2 solution. Continuous line represents the fitting of experimental data to eq 23. Parameters used for the fitting of experimental data are collected in Table 3.

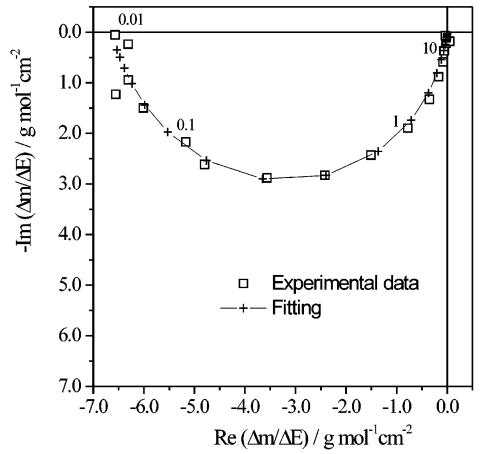

Figure 6. Ac-electrogravimetric transfer function of a PB film at $E = +0.100$ V vs SCE in NaCl 0.5 M and pH 2.2 solution. Continuous line represents the fitting of experimental data to eq 24. Parameters used for the fitting of experimental data are collected in Table 3.

metry are not identical, a good correlation between them can be observed. If values obtained from fitting in KCl (Table 2) and NaCl solutions (Table 3) are compared, the following are found:

(1) The value of $(1/G_e + 1/G_{c^+})$ is always larger in NaCl solutions. If this term is mainly attributed to the contribution of cations insertion/expulsion in the PB film, then it means that the insertion of sodium cations proves less favored. This difference can be explained by the fact that sodium cations are more hydrated in the outer solution, and therefore, the energy needed for the insertion is greater than that for the potassium cations. This fact is also corroborated by the dependence of the voltammetric peak potential on the cation present in the solution (Figure 2), $E_{p(K^+)} > E_{p(Na^+)}$.

(2) The dependence of $(1/G_e + 1/G_{c^+})$ on the potential gives values for the $\alpha = 0.39$ and $\beta = 0.26$ in this case. This difference is also consistent with the shape of voltammograms, where the anodic peak proves higher and thinner than the cathodic one (more irreversible than in KCl solutions).

(3) The value of the time constant, τ_{c^+}, is always greater in NaCl solutions than in KCl solutions, indicating that sodium cations move slower than potassium cations through the PB film. It should be considered that the hydrated radii of sodium cations in aqueous solutions is larger than the size of inner "zeolitic" channels in the PB structure (3.2 Å in diameter[56,57])

(4) Values of K_{c^+}/dG_{c^+} are very similar at the redox potential, $E°$, in NaCl ($E = 0.1$ V) and KCl ($E = 0.2$ V) solutions. And furthermore, at potentials $E° = +0.100$V and $E° = +0.200$V, these values are very similar in both solutions. The inverse of this relationship without considering the film thickness $-$ G_{c^+}/K_{c^+} has the physical meaning of the low frequencies limit of $\Delta C_i/\Delta E$ (ω)and can attributed to the derivative of the insertion law (eq 10) for K^+ and Na^+ cations.[31] Looking at the voltammogram of Figure 2, it is observed that the shape of anodic peaks and the currents are very similar, but only displaced 0.100 V. Then the same number of cations is expected to compensate electrical charge in both systems, and therefore derivatives of insertion laws are similar, because this parameter refers to the number of mols of cations that enters or leaves the film.

(5) Values for the $(K_e\sqrt{\tau_e})/dG_e$ parameter, that is associated to the electron transport through the film, are also very similar in films immersed in both solutions, but in this case, minimum values for this parameter are at 0.150 V in NaCl solutions and 0.200 V in KCl solutions.

(*c*) *CsCl Solutions.* Figure 7 shows data of ac-electrogravimetry in a CsCl solution at different potentials. The shape of this figure also corresponds to a semicircle on the third quadrant

TABLE 3: Dependence of Parameters Obtained from the Fitting of Impedance Data and Ac-Electrogravimetry Data to Eqs 23 and 24 for a PB Film Immersed in a NaCl 0.5 M Solution at Different Potentials against the SCE Reference Electrode.

	impedance				ac-electrogravimetry			
E (V)	$1/FG_e + 1/FG_{c^+}$ (Ω cm^2)	$K_{c^+}/G_{c^+}d$ (V cm^2 μmol^{-1})	τ_{c^+}	$(K_e\sqrt{\tau_e})/dG_e$ (V cm^2 s$^{1/2}$ μmol^{-1})	$1/FG_e + 1/FG_{c^+}$ (Ω cm^2)	$K_{c^+}/G_{c^+}d$ (V cm^2 μmol^{-1})	τ_{c^+}	$(K_e\sqrt{\tau_e})/dG_e$ (V cm^2 s$^{1/2}$ μmol^{-1})
0.00	45	4	1.4	4	60	4	0.7	1
0.05	19	3	0.5	2	26	3	0.5	1
0.10	10	3	0.3	1	13	3	0.4	1
0.15	7	4	0.2	1	10	5	0.2	1
0.20	9	8	0.2	2	13	8	0.1	1
0.25	15	14	0.2	3	17	14	0.2	3
0.30	25	18	0.2	7	38	21	0.2	8

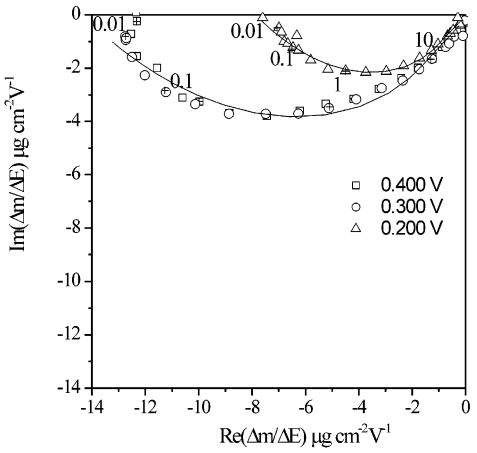

Figure 7. Ac-electrogravimetric transfer function of a PB film at $E = +0.200$, $+0.300$ V and $+0.400$ V vs SCE in CsCl 0.5 M and pH 2.0 solution. Continuous line represents the fitting of experimental data to eq 24. Parameters used for the fitting of experimental data are collected in Table 4.

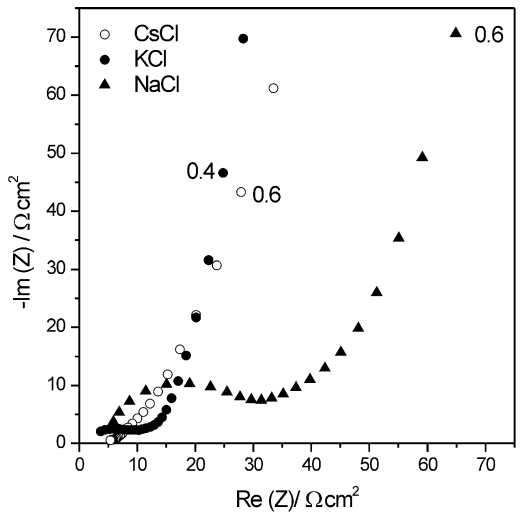

Figure 8. EIS presented as Nyquist plots of a PB film at $E = +0.300$ V vs SCE in NaCl 0.5 M and pH 2.2, KCl 0.5M pH = 2.0, and CsCl 0.5M pH = 2.0 solution.

that is interpreted as a main contribution of cations in the charge compensation process. In this case, the $F\,\Delta m/\Delta q$ relationship gives values on the order of 120 g mol^{-1} (<133 g mol^{-1}, corresponding to a pure Cs^+ participation) that implies a partial but small contribution of other species to the charge compensation process, perhaps hydrated protons or the exit of water molecules from the PB film when cesium cations are inserted.

Impedance spectra for this film in CsCl solutions also show an apparently similar shape to that in NaCl or KCl solutions (Figure 8). However, there are some differences that should be mentioned. EIS spectra do not show in the Nyquist plot the high frequencies semicircle associated to transfer charge resistances or to the $(1/G_e + 1/G_c)$ parameter in this model.

Table 4 collects values obtained from the fitting of experimental impedance spectra and ac-electrogravimetry dada to eqs 23 and 24. There are several points to be indicated. On one hand, these parameters are less dependent on the potential in CsCl solutions than in other aqueous salt solutions, as it could be expected looking at the voltammogram of Figure 2.

On the other hand, both K_c/G_cd and $(K_e\sqrt{\tau_e})/G_ed$ are 1 order of magnitude larger than in NaCl and KCl solutions. These parameters (interpreted as the inverse of the derivative of the insertion law) are fully consistent with the smaller values for the current in the voltammogram of Figure 2a in CsCl solution.

Values for time constants, τ_{c^+}, are slightly larger than those obtained in KCl solutions at the redox potential and similar to those obtained in NaCl solutions at the redox potential. According to this result, it seems that the voltammetric peaks are made wider by not only the rate of transport of cesium cations in the PB film but also values for the K/G parameters.

As it could be expected from the shape of impedance spectra, the parameters $1/(FG_{c^+} + FG_e)$ cannot be evaluated from impedance or ac-electrogravimetry data in CsCl solutions. That means that there is neither important resistance nor energetic barrier to the insertion of cations into the film. This result can be explained by considering that in PB films, this parameter depends on the necessity to dehydrate cations before entering the film. In this case, cesium cations easily lose their water, and therefore can be easily inserted in the PB film.

Conclusion

These results clearly show that the electrochemical behavior of PB films depends on the nature of the alkali cation present in the aqueous solution, and this dependence is related not only with the rate of transport of these species through the film but also with the easiness of insertion−expulsion of cations during the electrochemical processes.

The mass/electrical charge ratio during a voltammogram shows that all the studied cations enter or leave the PB film without water. This result is also confirmed by ac-electrogravimetry. It is clear that cations should also be hydrated into the PB film by inner water. Therefore, this process should be understood as a process that takes place at the film/solution interface and that consists of the cation dehydration before entering the film and a posterior hydration into the film.

This hypothesis of the previous dehydration can explain the dependence of peak potential during voltammograms, since the energy needed to dehydrate cations at this interface is the main energy barrier to the cations insertion or expulsion. This variation shows a good correlation with the variation of

TABLE 4: Dependence of Parameters Obtained from the Fitting of Impedance Data and Ac-Electrogravimetry Data to Eqs 23 and 24 for a PB Film Immersed in a CsCl 0.5 M Solution at Different Potentials against the SCE Reference Electrode

	impedance				ac-electrogravimetry			
E (V)	$1/FG_e + 1/FG_{c^+}$ (Ω cm^2)	$K_{c^+}/G_{c^+}\,d$ (V cm^2 μmol^{-1})	τ_{c^+}	$(K_e\sqrt{\tau_e})/dG_e$ (V cm^2 s$^{1/2}$ μmol^{-1})	$1/FG_e + 1/FG_{c^+}$ (Ω cm^2)	$K_{c^+}/G_{c^+}d$ (V cm^2 μmol^{-1})	τ_{c^+}	$(K_e\sqrt{\tau_e})/dG_e$ (V cm^2 s$^{1/2}$ μmol^{-1})
0.4		84	0.1	61		98	0.3	54
0.3		94	0.1	51		96	0.2	42
0.2		103	0.3	55		183	0.3	64

hydration enthalpies for these cations, which are smallest for cesium and largest for sodium cations ($\Delta H_{hyd,Cs^+} = -282$ KJ mol^{-1}) < ($\Delta H_{hyd,K^+} = -336$ KJ mol^{-1}) < ($\Delta H_{hyd,Na^+} = -444$ KJ mol^{-1}).

Another result that can be explained is the different shape of voltammetric peaks in the different aqueous salt solutions. In KCl solutions and also in CsCl solutions, currents for the cathodic and anodic peaks are similar, while in NaCl solutions, anodic peak is larger and narrower (peak current = 398 μA cm^{-2}, and half peak width = 176 mV) than the cathodic one (peak current = 307 μA cm^{-2} and half peak width = 276 mV). However, electrical charge enclosed is very similar in both peaks (4.9 mC cm^{-2} for the cathodic peak, and 4.8 mC cm^{-2} for the anodic one). A possible explanation for these differences can be found in the fact that hydrated sodium cations are larger than the zeolitic channels of the PB structure, and therefore, the degree of hydration of these cations is smaller when they are inserted in the film. Thus, the energy barrier to leave the film will be smaller than the energy needed to enter the film. That makes the cathodic peak wider and shorter than the anodic one in this solution.

In the case of Cs^+ cations, the energy needed to enter the film is very small (the reduction process starts at more positive potentials) but their mobility within the film is also smaller than the mobility of potassium and sodium and that causes the peak to be wider, even when the insertion process proves easier.

Then, the insertion−expulsion process during the electrochemical reaction can be postulated by

$$C^+\cdot(H_2O)_{x,soln} + <PB,H_2O> \rightleftarrows x(H_2O)_{soln} + <PB,C^+\cdot(H_2O)_{y,film}> \quad \text{(ii)}$$

where in KCl and CsCl solutions, x (degree of hydration in the solution) and y degree of hydration into the film are similar, but in NaCl solutions, $y < x$.

This hypothesis agrees also with other experimental results that prove that water molecules within the PB film play a very important role during electrochemical processes.[20]

The model hereby analyzed, which considers both potential drop at the electrode/film and potential drop at the film/solution, has proved more suitable and reproduces better experimental impedance and ac-electrogravimetry data than the possibility of considering that two cations participate during the charge compensation process.

Acknowledgment. J.J. García-Jareño acknowledges financial support from Ministerio de Ciencia y Tecnología (Spain), Prog. Ramón y Cajal. D. Giménez-Romero acknowledges an FPI fellowship from Generalitat Valenciana. Part of this work has been supported by Ministerio de Ciencia y Tecnología MAT 2000-100-P4-03.

References and Notes

(1) De Levie, R. *Electrochem. Eng.* **1967**, *6*, 329.
(2) Rubinstein, I.; Risphon, J.; Gottesfeld S. *J. Electrochem. Soc.* **1986**, *133*, 729.
(3) Amemiya, T.; Hashimoto, K.; Fujishima, A. *J. Phys. Chem.* **1993**, *97*, 9187.
(4) Lang, G.; Ujvári, M.; Inzelt, G. *Electrochim. Acta* **2001**, *46*, 4159.
(5) Armstrong, R. D.; Lindholm, B.; Sharp, M. *J. Electroanal. Chem.* **1987**, *235*, 169.
(6) Vorotyntsev, M. A.; Daikhin, L. I.; Levi, M. D. *J. Electroanal. Chem.* **1994**, *364*, 37.
(7) Mathias, M. F.; Haas, O. *J. Phys. Chem.* **1992**, *96*, 3174.
(8) Neff, V. D. *J. Electrochem. Soc.* **1978**, *125*, 886.
(9) Itaya, K.; Shibayama, K.; Akahoshi, H.; Toshima, S. *J. Appl. Phys.* **1982**, *53*, 804.
(10) Itaya, K.; Ataka, T.; Toshima, S. *J. Am. Chem. Soc.* **1982**, *104*, 4767.
(11) Itaya, K.; Akahoshi, H.; Toshima, S. *J. Electrochem. Soc.* **1982**, *129*, 1498.
(12) Mortimer, R. J.; Rosseinsky, D. R. *J. Electroanal. Chem.* **1983**, *151*, 133.
(13) Mortimer, R. J.; Rosseinsky, D. R. *J. Chem. Soc., Dalton Trans.* **1984**, *9*, 2059.
(14) Feldman, B. J.; Melroy, O. *J. Electroanal. Chem.* **1987**, *234*, 213.
(15) Feldman, B. J.; Murray, R. W. *Inorg. Chem.* **1987**, *26*, 1702.
(16) García-Jareño, J. J.; Navarro-Laboulais, J.; Vicente, F. *Electrochim. Acta* **1996**, *41*, 835.
(17) Piela, P.; Wrona, P. K.; Galus, Z. *J. Electroanal. Chem.* **1994**, *378*, 159.
(18) Inove, H.; Yanagisawa, S. *J. Inorg. Nucl. Chem.* **1974**, *36*, 1409.
(19) García-Jareño, J. J.; Sanmatías, A.; Navarro-Laboulais, J.; Benito, D.; Vicente F. *Electrochim. Acta* **1998**, *43*, 235.
(20) García-Jareño, J. J.; Sanmatías, A.; Navarro-Laboulais, J.; Vicente, F. *Electrochim. Acta* **1998**, *43*, 395.
(21) García-Jareño, J. J.; Sanmatías, A.; Vicente, F.; Gabrielli, C.; Keddam, M.; Perrot, H. *Electrochim. Acta* **2000**, *45*, 3765.
(22) García-Jareño, J. J.; Navarro, J.; Roig, A. F.; Scholl, H.; Vicente, F. *Electrochim. Acta* **1995**, *40*, 1113.
(23) Oh, I.; Lee, H.; Yang, H.; Kwak, J. *Electrochem. Comm.* **2001**, *3*, 274.
(24) Kulesza, P. J. *J. Electroanal. Chem.* **1990**, *289*, 103.
(25) Cordoba-Torresi, S.; Gabrielli, C.; Keddam, M.; Takenouti, H.; Torresi, R. *J. Electroanal. Chem.* **1990**, *290*, 261.
(26) Bourkane, S.; Gabrielli, C.; Keddam, M. *Electrochim. Acta* **1989**, *34*, 1081.
(27) Bourkane, S.; Gabrielli, C.; Huet, F.; Keddam, M. *Electrochim. Acta* **1993**, *38*, 1023 and 1827.
(28) Gabrielli, C.; Keddam, M.; Nadi, N.; Perrot, H. *Electrochim. Acta* **1999**, *44*, 2095.
(29) . Gabrielli, C.; Keddam, M.; Nadi, N.; Perrot, H. *J. Electroanal. Chem.* **2000**, *485*, 101.
(30) . Gabrielli, C.; Keddam, M.; Perrot, H.; Pham, M. C.; Torresi, R. *Electrochim. Acta* **1999**, *44*, 4217.
(31) Gabrielli, C.; García-Jareño, J. J.; Keddam, M.; Perrot, H.; Vicente, F. *J Phys. Chem. B* **2002**, *106*, 3182.
(32) Gabrielli, C.; García-Jareño, J.; Perrot, H. *ACH - Models Chem.* **2000**, *137*, 269.
(33) Kim, K.; Jureviciute, I.; Bruckenstein, S. *Electrochim. Acta* **2001**, *46*, 4133.
(34) Yang, H.; Kwak, J. *J. Phys. Chem. B* **1997**, *101*, 774.
(35) Yang, H.; Kwak, J. *J. Phys. Chem. B* **1997**, *101*, 4656.
(36) Yang, H.; Kwak, J. *J. Phys. Chem. B* **1997**, *102*, 1982.
(37) Lee, H.; Yang, H.; Kim, Y. T.; Kwak, J. *J. Electrochem. Soc.* **2000**, *147*, 3801.
(38) Benito, D.; Gabrielli, C.; García-Jareño, J. J.; Keddam, M.; Perrot, H.; Vicente, F. *Electrochem. Comm.* **2002**, *4*, 613.
(39) Raistrick, I. D. *Electrochim. Acta* **1990**, *35*, 1579.
(40) Rubinstein, I.; Sabatini, E.; Rishpon, J. *J. Electrochem. Soc.* **1987**, *134*, 3078.
(41) Sauerbrey, G. *Z. Phys.* **1959**, *155*, 206.

(42) García-Jareño, J. J.; Gabrielli, C.; Perrot, H. *Electrochem. Comm.* **2000**, *2*, 195.
(43) Macdonald, J. R. *Solid State Ionics* **1992**, *58*, 97.
(44) Vicente, F.; Roig, A.; García Jareño, J. J.; Sanmatías, A. *Procesos electródicos del Nafión y del Azul de Prusia/Nafion sobre electrodo transparente óxido de Indio-Estaño: Un modelo de electrodos multicapa.* 2001 ISBN 84-931188-6-9, Moliner 40, Burjassot (Valencia).
(45) García-Jareño, J. J.; Navarrro-Laboulais, J.; Sanmatías, A.; Vicente, F. *Electrochim. Acta* **1998**, *43*, 1045.
(46) García-Jareño, J. J.; Sanmatías, A.; Benito, D.; Navarro-Laboulais, J.; Vicente, F. *Int. J. Inorg. Mat.* **1999**, *1*, 343.
(47) Chen, S.-M. *J. Electroanal. Chem.* **2002**, *521*, 29.
(48) Bácskai, J.; Martinusz, K.; Czirók, E.; Inzelt, G.; Kulesza, P. J.; Malik, M. A. *J. Electroanal. Chem.* **1995**, *385*, 241.
(49) Malik, M. A.; Miecznikowski, K.; Kulesza, P. J. *Electrochim. Acta* **2000**, *45*, 3777.
(50) Lasky, S. J.; Buttry, D. A. *J. Am. Chem. Soc.* **1988**, *110*, 6258.
(51) Chen, L.-C.; Ho,K.-C. *J. Electrochem. Soc.* **2002**, *149*, E40.
(52) Nguyen, P. H.; Paasch, G. *J. Electroanal. Chem.* **1999**, *460*, 63.
(53) Albery, W. J.; Elliott, C. M.; Mount, A. R. *J. Electroanal. Chem.* **1990**, *288*, 15.
(54) Ren, X.; Pickup, P. G. *J. Chem. Soc., Faraday Trans.* **1993**, *89*, 321.
(55) Buck, R. P.; Mundt, C. *J. Chem. Soc., Faraday Trans.* **1996**, *92*, 3947.
(56) Robin, M. B.; Day, P. *Adv. Inorg. Chem. Radiochem.* **1967**, *10*, 247.
(57) Seifer, G. B.; Russ, J. *Inorg. Chem.* **1962**, *7*, 621.